DOI: 10.1515/adms-2016-0008

Z. Ławrynowicz

University of Science and Technology, Mechanical Engineering Faculty, Department of Materials Science and Engineering, Av. Kaliskiego 7, 85-796 Bydgoszcz, Poland
lawry@utp.edu.pl

KINETICS OF THE BAINITE TRANSFORMATION IN AUSTEMPERED DUCTILE IRON ADI

ABSTRACT

The aim of the present research is to check an analytical model of the kinetics of bainite transformation that will enable the producers of ADI to optimise the microstructure and mechanical properties and minimise the expensive and extensive experimental trials. A combination of thermodynamics and kinetic theory was used successfully to estimate the evolution of bainite as a function of temperature, time, chemical composition and austenite grain size and predict the processing window in austempered ductile iron using a bainite transformation model developed previously for high silicon steels. The results of the present research show that the bainitic model developed for high silicon steels is applicable for calculations of the processing window for ADI.

Keywords: *kinetics of bainite transformation, austempered ductile iron ADI*

INTRODUCTION

Austempered Ductile Iron (ADI) compared to traditional ductile cast iron has more than twice the strength at comparable ductility [1,2,3]. However, to obtain optimal mechanical properties of ADI the isothermal transformation process should produce the desired bainitic microstructure. The desired microstructure of ADI, from the viewpoint of good mechanical properties, consists of a mixture of bainitic ferrite and carbon-enriched retained austenite called ausferrite [1,3,4] and spheroidal graphite. The microstructure has to be free from undesirable phases as precipitation of carbide, pearlite, and martensite, which in practice is difficult to achieve due to the high heterogeneity of the metal matrix. The time of isothermal transformation should provide a corresponding fraction of the bainitic ferrite, which in turn leads to an adequate carbon enrichment of the residual austenite which enhances its stability after cooling to room temperature. However, longer time of bainitic transformation leads to the decomposition of residual austenite to a mixture of ferrite and carbide [4] which worsen the mechanical properties. Elliott and Darwish [5,6,7] defined the processing window as a time and temperature range in which the mechanical properties of cast iron meet the requirements of ASTM A897M: 1990 [8].

The process of bainite isothermal transformation generally consists of two steps [9,10]. The end of the stage I corresponds to the maximum fraction of bainitic ferrite and carbon-enriched residual austenite. Stage II starts the precipitation of carbide from austenite. The time interval between these stages is a processing window (Fig. 1). The processing window on the

one hand, consists of the area between the bainitic transformation start temperature B_S, and the martensitic transformation start temperature, M_S. The determination of a processing window is associated however, with considerable experimental work and thus high cost.
Thus, the analytical estimation of processing window based on the kinetics of bainitic transformation seems to be very beneficial and it is a primary objective of this study.

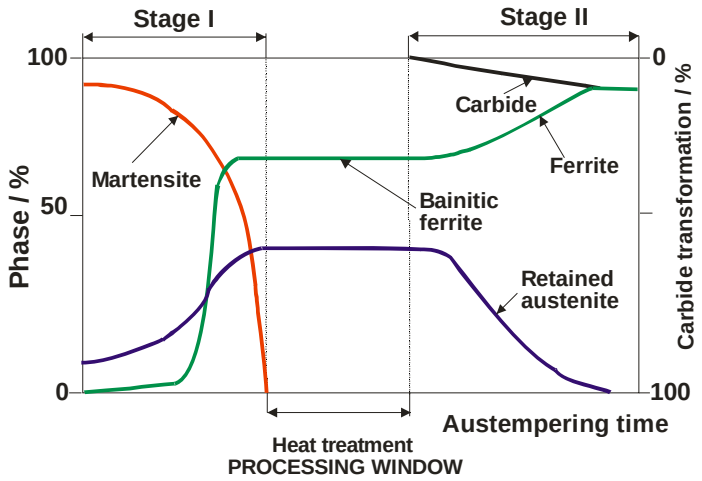

Fig. 1. Diagram showing the development of microstructure during isothermal bainitic transformation together with the illustration of processing window. Martensite is present, when the samples were cooled to room temperature before bainitic transformation was stopped (the end of stage I)

MATERIAL

The study involved unalloyed ductile iron ADI with the chemical composition given in Table 1.

Table 1. *Chemical composition of the tested ductile cast iron ADI, weight %*

C	Si	Mn	P	S	Mg	Cr	Ni	Mo
3.21	2.57	0.28	0.061	0.01	0.024	0.036	0.098	0.015

After casting it was found that the matrix consists of 40% ferrite and 60% pearlite, while the content of graphite nodules in the matrix was 11.5%. The bainitic and martensitic start temperatures were calculated in accordance with the [11-14] and its equal: $B_S = 437^oC$ and $M_S = 245^oC$.

The carbon content in austenite before and during the isothermal transformation was determined by X-ray diffractometer. A detailed description of the method of measurement is given in [15]. The dilatometrically determined temperature of the transformation $\alpha \rightarrow \gamma$ during the warm-up was $Ac_{1,2} = 827^oC$ [15,16]. Thus, it was found that after quenching from austenitising temperature 830°C the measured concentration of carbon in austenite was 0.65% C and that value was taken for further calculation.

ANALYSIS OF TRANSFORMATION MECHANISM

Table 2 shows the measured carbon concentration in retained austenite and the estimated parameters of the phase equilibrium diagram of the tested ductile cast iron ADI. Fig. 2 shows calculated for different thermodynamic conditions the phase diagram of investigated cast iron and measured carbon contents in austenite. It is useful to define a number of thermodynamic parameters of the diagram. The curve T_0 represents the location of all points on the diagram: temperature - carbon concentration, where austenite and ferrite (stress free) having the same chemical composition has also the same free energy. Hence, the austenite, which has a carbon concentration exceeding the value determined by the curve T_0 cannot be transformed by diffusionless mechanism. The growth of bainite is accompanied by a change in shape, which is characterized by the invariant plane strain with high shear component. The strain induced in the austenite at the time when it accommodates deformation was estimated as a value of 400 J/mol [17,18]. Line modified to account for the strain energy is called T_0' curve. A'_3 curve represents the interface boundary $(\alpha+\gamma)/\gamma$ in paraequilibrium conditions, ie. there is existence of a balance between ferrite and austenite (stress free) and the ratio of content of substitutional alloying elements to iron is the same in both phases [19,20]. Element ΔG_m^0 is the initial value of maximum possible free energy change on nucleation.

Table 2. *Measured concentration of carbon in retained austenite, and the estimated parameters of the phase equilibrium diagram of the ADI*

T_i, ^oC	ΔG_m^0 *J/mol*	A'_3	x_{T_0} *Mole*	$x_{T_0'}$ *mole*	Measured carbon contents in austenite, x_γ, after isothermal holding for 15 and 240 minutes	
					15 minutes	240 minutes
250	-2585	0.1805	0.0708	0.0555	0.0288	0.0620
300	-2316	0.1670	0.0645	0.0491	0.0368	0.0567
350	-1891	0.1507	0.0547	0.0408	0.0687	0.0727
400	-1611	0.1352	0.0471	0.0337	0.0545	0.0673
500	-999	0.1018	0.0325	0.0217		
600	-460	0.0662	0.0218	0.0095		
700	-70	0.0342	0.0122	-		

Fig. 2 allows comparison of the measured concentration of carbon in austenite in relation to the desired concentration if bainite formation has stopped after the carbon concentration of the austenite reaches boundaries A'_3, T_0 or T_0'. These boundaries are understood as defined by Christian and Edmonds in [11].

In presented diagram the reaction is found to stop when the average carbon concentration of the residual austenite is closer to the T_0 and T_0' curves than the A'_3 boundary. The presented results can be explained when it is assumed that bainitic ferrite grows without diffusion, but any excess of carbon is soon afterwards rejected into the residual austenite by diffusion [13,14,21]. This makes more difficult for subsequent bainitic ferrite to grow, when the austenite becomes stabilised by increased carbon concentration. The maximum extent to which the bainite reaction can proceed is therefore determined by the composition of the residual austenite. A stage where diffusionless growth becomes thermodynamically impossible and the formation of bainitic ferrite terminates is where the carbon concentration

of the austenite reaches the T_0' or T_0 curves which are based on the diffusionless transformation.

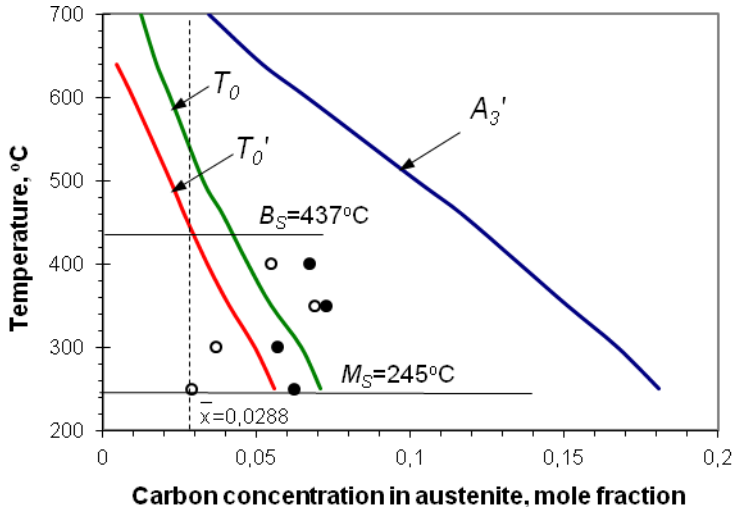

Fig. 2. The calculated phase boundaries A'_3, T_0 and T_0' for the investigated ADI together with all the experimental data of the measured carbon contents of the austenite. Light dots mean the determined carbon concentration in austenite at the beginning of isothermal transformation at 400, 350, 300 and 250°C (15 minutes), while the dark dots at the end of the heating process after 240 minutes

Thus, it is found experimentally that the transformation to bainite does indeed stop close to the T_0 boundary (Fig. 2). The thermodynamic restriction imposed by the T_0 curve on the extent of bainite transformation can result in the formation of pools of retained austenite with a coarse, blocky morphology, Fig. 3.

Fig. 3 shows a typical microstructure of ADI austenitised at 830°C and austempered at 350°C for 30 min. and reveals the morphology of bainite which consists of blocky regions of retained austenite and fine laths of bainitic ferrite [15]. Fine dispersed particles of carbides can be seen inside bainitic ferrite laths (Fig. 3b).

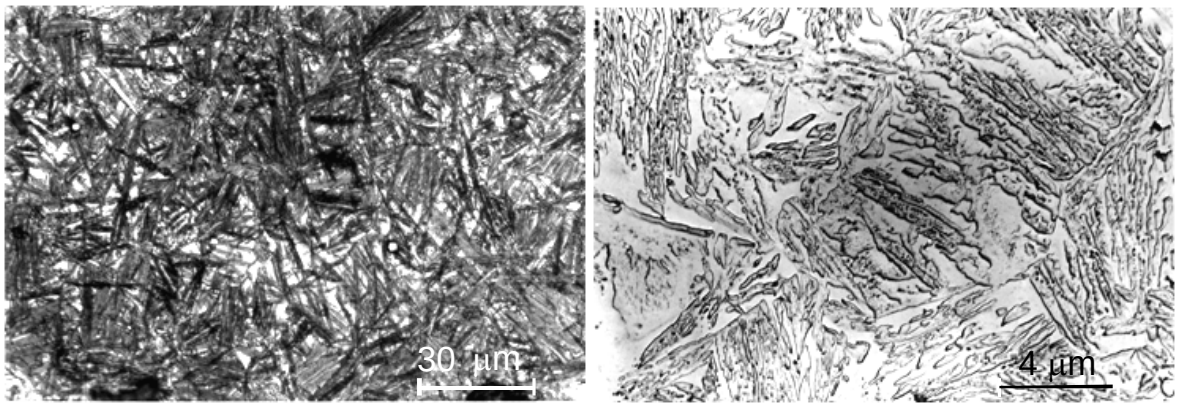

a) b)

Fig. 3. Microstructure of cast iron ADI austenitised at 830°C and austempered at 350°C for 30 min., a) optical metallography revealing the sheaves of lower bainite (black) and pools of retained austenite (white), nital, b) carbon replica

To estimate the limits of a processing window the mathematical model of the kinetics of bainitic transformation was used, allowing the determination of the degree of transformation in time. The model is based on the bainite transformation at high silicon steels (> 1.5% silicon) in which the release of carbides is inhibited [20]. The use of this model is possible in the case of bainitic ferrite displacive growth mechanism, followed by the removal of carbon from ferrite to retained austenite.

The model was adjusted by taking into account a change in bainite laths size with temperature. According to [22,23] a linear relationship between temperature and width (u_w) of bainite lath is given by:

$$u_w = 0{,}001077T - 0{,}2681 \tag{1}$$

where: T is the temperature in °C, and u_w is lath width in μm.

Fig. 4 shows the model prediction, taking into account the change in u_w with isothermal transformation temperature.

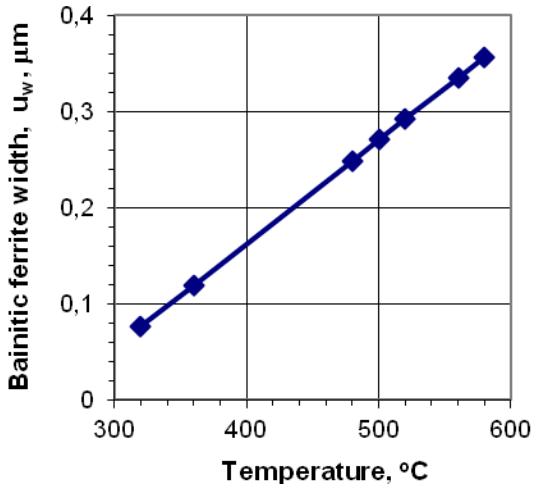

Fig. 4. Calculated change of bainitic ferrite lath with isothermal transformation temperature

KINETICS OF BAINITE TRANSFORMATION

There are numerous models of the kinetics of bainitic transformation, but only one is based on the physical mechanism of transformation [22,23,24]. According to experimental data (Table 2, Fig. 2,3) it is understood that the mechanism of bainite growth is diffusionless, with partitioning of carbon in the residual austenite, which occurs shortly after the growth of bainitic laths is arrested. This finding has important implications, that transformation stops when diffusionless growth becomes thermodynamically impossible to sustain. The model also takes into account:

-the effect of carbon partitioning on free energy change,
-the phenomenon of autocatalysis,
- austenite grain size.

The effect of these factors is not discussed here, but the speed with we get a the relative fraction of bainite is determined by:

$$\frac{d\xi}{dt} = \frac{uK_1}{\theta}(1-\xi)(1+\beta\theta\xi)\exp\left[-\frac{K_2}{RT}\left(1+\frac{\Delta G_m^0}{r}\right)+\Gamma_2\xi\right] \tag{2}$$

$$\text{where: } \Gamma_2 = \frac{K_2\left(\Delta G_m^0 - G_N\right)}{rRT} \tag{3}$$

Determination of nucleation rate is based on the linear dependence of activation energy on chemical driving force ΔG_m, and on the assumption that the rate of nucleation at the Widmanstätten start temperature W_S is constant for all alloys regardless of their chemical composition.

The influence of carbon partitioning on free energy change was included by the assumption that the driving force varies linearly with the progress of transformation between the starting value ΔG_m^0 and the final value G_N when the transformation ends.

The expression ΔG_m^0 is the initial value of the maximum possible change of the nucleation free energy. The universal function of nucleation, G_N, represents the minimum driving force required to initiate nucleation of ferrite by shear mechanism. During transformation, it becomes necessary to take into consideration reduction of driving force due to carbon enrichment of the retained austenite.

The bainite transformation kinetics model takes into account also the effect of autocatalysis - ie. increase the density of nucleation sites with an increase in the volume fraction of ferrite.

Autocatalysis factor β, as in the theory of martensitic transformation, describes the extent to which the formation of one lath of bainite stimulates the emergence of other laths. It has been established that autocatalysis factor β is a function of the average carbon concentration in the alloy $\bar{x}$, since the increase in the carbon content in the austenite causes the reduction in the driving force for the diffusionless transformation and thus inhibits the autokatalysis [22,23].

The density of nucleation sites on the grain borders should be proportional to the surface of the grain boundaries in relation to their volume. Therefore, the term K_1 is inversely proportional to the average size $\bar{L}$ of the measured austenite grains.

The phenomenon of incomplete reaction is taken into account by the maximum volume fraction of formed bainite θ, which is calculated by using the Lever Rule applied to the curve T_0' (or T_0) of the phase diagram in paraequilibrium conditions [24-27]:

$$\theta = \frac{x_{T_0'} - \bar{x}}{x_{T_0'} - x_\alpha} \tag{4}$$

The average carbon concentration in the alloy ($\bar{x}$) expressed as a mole fraction, $x_{T_0'}$ - corresponds to a carbon concentration on the line T_0' (similarly x_{T_0} is the concentration of carbon on the T_0 line), and x_α is estimated concentration of carbon in ferrite. The carbon

content of bainitic ferrite is taken as x_α = 0,00139mol. (0.03 wt. %) [13]. Calculations x_{T_0}, $x_{T_0'}$, x_α and ΔG_m^0 performed as in [4,10,17]. And the next symbols:

β - autocatalysis factor, $\beta = \lambda_1(1 - \lambda_2 \bar{x})$

λ_1, λ_2 - empirical constans

ξ - normalised volume fraction of bainite $\xi = \dfrac{\nu}{\theta}$

K_1 - function of austenite grain size $K_1 = \left(\bar{L} K_1'\right)^{-1}$

K_1, K_2 - empirical constant

r - constant

R - gas constant

t - time (s)

T - temperature (^{0}C)

The influence of all these factors is taken into account in the modelling of the kinetics of bainite transformation, so after integration of equation (2) the time until an adequate degree of bainitic transformation was determined by [22]:

$$t = \frac{\exp(C)}{A(B+1)} \left\{ \begin{array}{l} \exp(E)\left(\ln|1 + B\xi| + f\left(-(E + D\xi)\right) - f\left(-E\right)\right) \\ -\exp(-D)\left(\ln(1-\xi) + f\left(D(1-\xi)\right) - f\left(D\right)\right) \end{array} \right\} \tag{5}$$

where:

$$A = \frac{uK_1}{\theta},\ B = \beta\theta,\ C = \frac{K_2}{RT}\left(1 + \frac{\Delta G_m^0}{r}\right),\ D = \Gamma_2,\ \Gamma_2 = \frac{K_2\left(\Delta G_m^0 - G_N\right)}{rRT},\ E = \frac{D}{B},\ t - \text{time (s)},$$

$$f(x) = \frac{x}{1 \times 1!} + \frac{x^2}{2 \times 2!} + \frac{x^3}{3 \times 3!} + \ldots$$

Equation (5) was used to predict the time (t) required to achieve a specific volume fraction of bainite formed at a given temperature. The time can be anticipated for the various degrees of transformation up to a maximum value (the concentration of carbon in austenite reaches x_{T_0} or $x_{T_0'}$), but has not yet started precipitation of cementite. Then there would be in the cast iron ADI microstructure of ausferrite, which has optimal mechanical properties.

Because in the range of the upper bainite precipitation of cementite occurs, as indicated by the calculated phase diagram of tested cast iron ADI (see Fig. 2), and this leads to an increase in the degree of transformation, than the maximum volume fraction of the bainitic ferrite was determined, which is a function of the temperature and the amount of precipitated cementite in bainite [15]:

$$\theta = \frac{x_{To} - \bar{x}}{x_{To} - x_\alpha - x_C} \tag{6}$$

where x_C is the amount of carbon stored in the carbides (in cementite). Table 3 shows the time of the termination of processing window for different austenite grain size.

The results of the calculation of the time required to obtain a specific of the degree of bainite transformation in cast iron ADI (5% and 95%), depending on different average

austenite grain size 20, 40 and 80 μm, and precipitated 1% cementite are shown in Figs 5-7. For the calculation of the degree of transformation in Fig. 5-7 was assumed that the carbon concentration in austenite at the time when transformation seems to stop equals x_{To}.

Table 3. *Time of the termination of processing window, minutes*

Mean grain size, d μm	Temperature of izothermal transformation, °C			
	250	300	350	400
	Time of the termination of processing window, minutes			
20	28	33	22	18
40	56	66	45	35
80	112	132	88	70

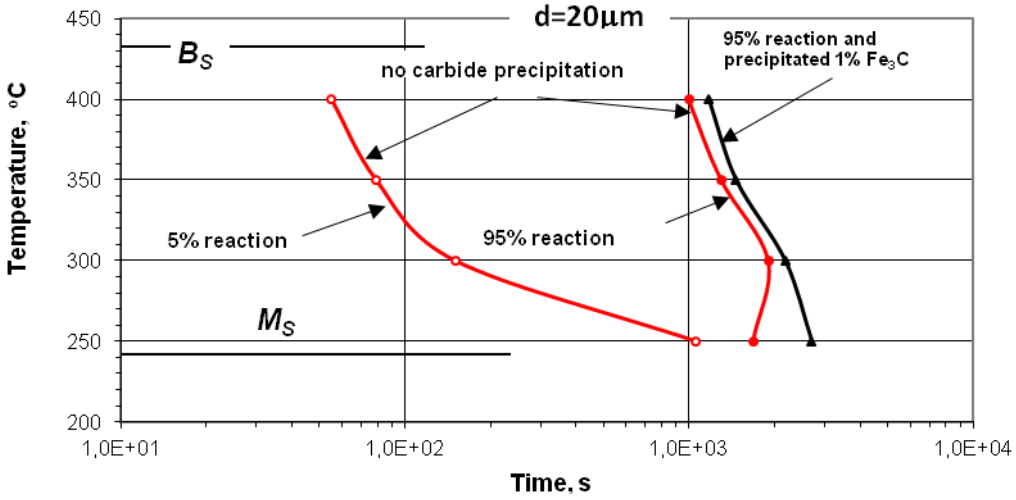

Fig. 5. The calculated part of the TTT diagram for ductile iron ADI with 5% and 95% volume fraction of bainitic ferrite for austenite mean grain size d = 20 μm when is only ausferrite without cementite. Line on the right indicates time of transformation when 1% of cementite precipitated (the beginning of stage II)

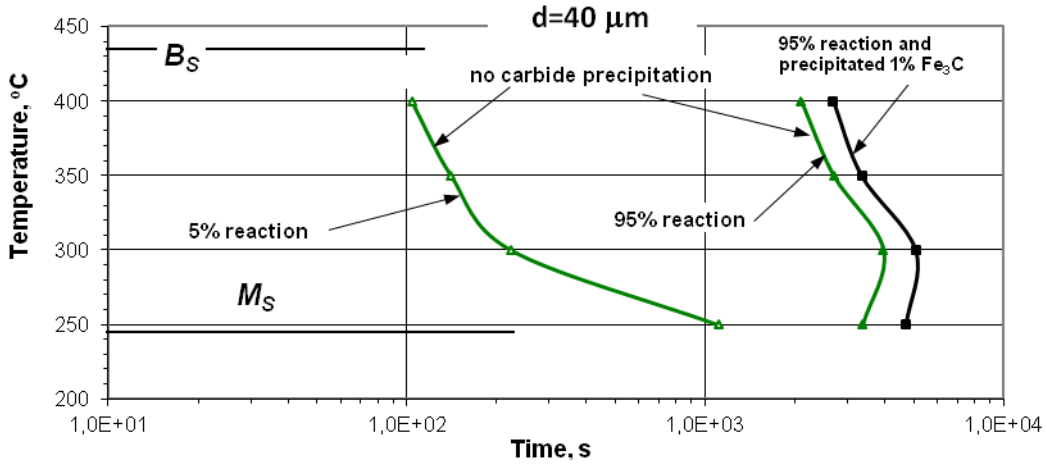

Fig. 6. The calculated part of the TTT diagram for ductile iron ADI with 5% and 95% volume fraction of bainitic ferrite for austenite mean grain size d = 40 μm when is only ausferrite without cementite. Line on the right indicates time of transformation when 1% of cementite precipitated (the beginning of stage II)

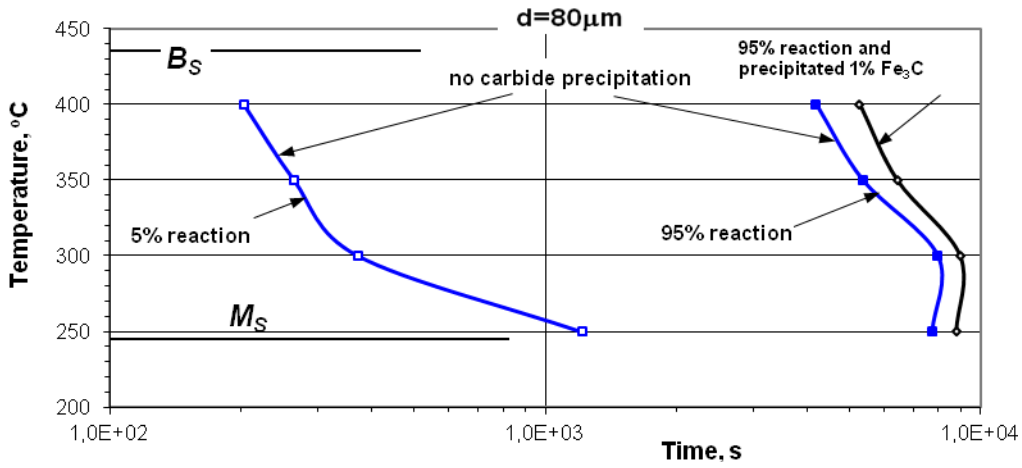

Fig. 7. The calculated part of the TTT diagram for ductile iron ADI with 5% and 95% volume fraction of bainitic ferrite for austenite mean grain size d = 80 μm when is only ausferrite without cementite. Line on the right indicates time of transformation when 1% of cementite precipitated (the beginning of stage II)

CONCLUSIONS

1. It is possible to model the kinetics of bainite transformation in ADI cast iron using the theory of thermodynamics and kinetics of the bainite transformation, designed for high-silicon steels.
2. When the beginning of cementite precipitation means the end of a processing window, it is possible to estimate the processing time interval depending on the heat treatment parameters, the chemical composition and grain size.

REFERENCES

1. Pietrowski S., Nodular cast iron of bainitic ferrite structure with austenite or bainitic structure. Archives of Materials Science. 18 (1997) 253-273 (in Polish).
2. Chang L.C., Carbon content of austenite in austempered ductile iron. Scripta Materialia. 39 (1998) 35-38.
3. Guzik S.E., Austempered cast iron as a modern constructional material. Inżynieria Materiałowa. 6 (2003) 677-680 (in Polish).
4. Ławrynowicz Z., Dymski S., Analysis of carbon diffusion during bainite transformation in ADI. Archives of Foundry Engineering. 7 (2007) 87-92.
5. Davis J.R. in "ASM speciality handbook", (ed. J.R. Davis) (1996), 192-204 Metals Parks, OH, American Society for Metals.
6. Darwish N., Elliott R.: Austempering of low manganese ductile irons. Materials Science and Technology. 9 (1993) 572-585.
7. Elliott R.: The role of research in promoting austempered ductile iron. Heat Treatment of Metals. 23 (1997) 55-59.

8. ASTM standard A897M-90metric, ASTM, Philad. PA, USA, (1990) 560-565.
9. Soliman M., Palkowski H., Development of the low temperature bainite. Archives of Civil and Mechanical Engineering. 16 (2016) 403-412.
10. Ławrynowicz Z., Dymski S.,: Analysis of carbon partitioning during ausferritic reaction in ADI. Archives of Foundry Engineering. 8 (2008) 69-74.
11. Christian J.W., Edmonds D.V., Int. Conf. on Phase Transformations in Ferrous Alloys, A.R. Marder and J.I. Goldstein, eds., ASM, Metals Park, OH, (1984) 293-326.
12. Takahashi M., Bhadeshia H.K.D.H., A Model for the Microstructure of Some Advanced Bainitic Steels. Materials Transaction, JIM, 32 (1991) 689-696.
13. Ławrynowicz Z., Transition from upper to lower bainite in Fe-Cr-C steel. Materials Science and Technology. 20 (2004) 1447-1454.
14. Bhadeshia H.K.D.H., Christian J.W., Bainite in Steels. Metallurgical Transactions A. 21A (1990) 767-797.
15. Dymski S., Kształtowanie struktury i właściwości mechanicznych żeliwa sferoidalnego podczas izotermicznej przemiany bainitycznej, Rozprawy nr 95, ATR Bydgoszcz, (1999)
16. Ławrynowicz Z., Dymski S., Decarburisation of ferrite laths during bainite reaction in ADI. Journal of Polish CIMAC. 4 (2009) 65-72.
17. Bhadeshia H.K.D.H., Bainite in Steels. Institute of Materials, 1-458, London, (1992).
18. Ławrynowicz Z., Carbon partitioning during bainite transformations in low alloy steels. Materials Science and Technollogy. 18 (2002) 1322-1324.
19. Matas S.J., Hehemann RF., The structure of bainite in hypoeutectoid steels. Trans AIME, (1961) 179–85.
20. Bhadeshia H.K.D.H., Edmonds D.V., The mechanism of bainite formation in steels. Acta Metallurgica. 28 (1980) 1265–1273.
21. Bhadeshia H.K.D.H.: Diffusion of carbon in austenite. Metal Science. 15 (1981) 477-479.
22. Chester N.A., Bhadeshia H.K.D.H., Mathematical Modelling of Bainite Transformation Kinetics. Journal de Physique. C5 7 (1997) 41-46.
23. Ławrynowicz Z., Przemiana bainityczna: matematyczne modelowanie kinetyki przemiany, Zeszyty Naukowe Politechniki Poznańskiej, Budowa Maszyn i Zarządzanie Produkcją. 1 (2004) 35-46.
24. Bhadeshia H.K.D.H., Bainite in Steels, Institute of Materials, 1-458, London, (1992).
25. Ławrynowicz Z., Carbon diffusion during bainite reaction in Fe-Cr-Si-C steel, 11th International Symposium on Advanced Materials ISAM-2009, Islamabad, Pakistan, 09-23. (2009).
26. Soliman M., Ibrahim H., Nofal A., Palkowski H., Thermo-mechanically processed dual matrix ductile iron produced by continuous cooling transformation. Journal of Materials Processing Technology. 227 (2016) 1-10.
27. Soliman M., Nofal A., Palkowski H., Alloy and process design of thermo-mechanically processed multiphase ductile iron. Materials & Design. 87 (2015) 450-465.